Biosensors and Bioelectronics: X 14 (2023) 100363

Contents lists available at ScienceDirect

Biosensors and Bioelectronics: X

journal homepage: www.journals.elsevier.com/biosensors-and-bioelectronics-x

Highly fluorescent nitrogen-doped carbon dots derived from jengkol peels (*Archindendron pauciflorum*) by solvothermal synthesis for sensitive Hg^{2+} ions detection

Aniza Salviana Prayugo [a], Marpongahtun [b,c,*], Saharman Gea [b], Amru Daulay [a], Mahyuni Harahap [d], Jonathan Siow [e], Ronn Goei [f], Alfred Iing Yoong Tok [f]

[a] Postgraduate School, Department of Chemistry, Faculty of Mathematics and Natural Sciences, Universitas Sumatera Utara, Jl. Bioteknologi No.1, Medan, 20155, Indonesia
[b] Department of Chemistry, Faculty of Mathematics and Natural Sciences, Universitas Sumatera Utara, Jl. Bioteknologi No. 1, Medan, 20155, Indonesia
[c] Cellulosic Functional Material-Research Center, Universitas Sumatera Utara, Jalan Bioteknologi No. 1, Kampus USU, Padang Bulan, 20215, Sumatera Utara, Indonesia
[d] Department of Chemistry, Faculty of Science Technology and Information, Sari Mutiara Indonesia University, Jl. Kapten Muslim No. 79, Medan, 20124, Indonesia
[e] School of Chemistry, Chemical Engineering and Biotechnology, Nanyang Technological University, 62 Nanyang Drive, 637459, Singapore
[f] School of Material Science and Engineering, Nanyang Technological University, 50 Nanyang Avenue, 637335, Singapore

ARTICLE INFO

Keywords:
Carbon dots
Jengkol peels
Solvothermal
Nitrogen-doped
Hg^{2+} detection
Fluorescence sensing

ABSTRACT

A facile synthesis method involving a one-step solvothermal method is demonstrated in producing fluorescent nitrogen-doped carbon dots (N-CDs) by employing biomass waste (Jengkol peels) and ethylenediamine as a source for carbon and nitrogen. The synthesized N-CDs are spherical nanoparticles with an average size of 4.495 nm, exhibit solubility in water, emit bluish-green fluorescence and a high quantum yield of up to 42%. By using UV–Visible, FTIR, XPS, HR-TEM and Photoluminescence analysis, the as-prepared N-CDs were verified. We demonstrate that nitrogen doping increases fluorescence emission intensity to its radiative recombination of the $\pi - \pi^*$ transitions at C═C and $n - \pi^*$ at C═O or C═N. an optimized excitation at 370 nm, the N-CDs exhibited strong PL emission at 522 nm. Under optimized conditions, N-CDs can be used to detect Hg^{2+} ions based on quenched fluorescence phenomenon. The result reveals excellent selectivity and sensitivity to Hg^{2+} ions with a detection range of 0.5 μM–4.5 μM. The resulting N-CDs may be used for detecting Hg^{2+} ions in cosmetics and tap water.

1. Introduction

Carbon dots (CDs) are dimension zero quasi-spherical carbon nanoparticle fluorescence materials with a size <10 nm, initial discovery in 2004 by the purification of carbon nanotubes (X. Xu et al., 2004). The advantages of CDs over quantum dots in semiconductors and organic dyes include their good photostability, high QY, minimal cytotoxicity, small size, low cost, easy surface functional ability, dependent fluorescence excitation wavelength, and simple tuning of the luminescence according to the application used, which makes them ideal for in various fields including optoelectrical sensing (Alkian et al., 2022), antibacterial (Pramudita et al., 2022), biomedicine (Zhu et al., 2022), and smart window (Goei et al., 2022).

CDs can be synthesized by various methods, including such as laser ablation(Kaczmarek et al., 2021), arch discharge (Chao-Mujica et al., 2021), pyrolysis (Marpongahtun et al., 2023), and nitric acid/sulfuric oxidation (González-González et al., 2022) methods. These methods had drawbacks, including complicated synthesis techniques, harsh climate, low quantum yields, high cost, environmental damage, rarely these techniques utilized to synthesized CDs from organic materials, and a time-consuming process to remove too much acid (Kang et al., 2020). While the microwave irradiation method can help reduce reaction time, its high energy consumption could be a drawback (Villalba-Rodríguez et al., 2022). Solvothermal methods are attractive for researchers because they may involve one step during synthesis, are low cost, are effective in regulating nanomaterials structure, and require simple equipment (Kang et al., 2020).

Recent developments have seen the utilization of waste biomass rich

* Corresponding author. Department of Chemistry, Faculty of Mathematics and Natural Sciences, Universitas Sumatera Utara, Jl. Bioteknologi No. 1, Medan, 20155, Indonesia.
E-mail address: marpongahtun@usu.ac.id (Marpongahtun).

https://doi.org/10.1016/j.biosx.2023.100363
Received 15 February 2023; Received in revised form 17 April 2023; Accepted 29 May 2023
Available online 20 June 2023

in phytochemicals as a carbon source for the synthesis of CDs (Dhanush et al., 2022). Jengkol peels (*Archindendron pauciflorum*) is a biomass waste that contains phytochemical compounds such as flavonoids, phenols, saponins and tannins (Rahmayanti et al., 2022). In addition, it also contains hemicellulose, cellulose, pectin, lignin (Wardani et al., 2020), and jengkolat acid (Nadira Hurairah et al., 2023). The large amount of jengkol peels waste that is not suitable for consumption and has no economic value resulting from traditional markets or households will cause environmental pollution, including the smell of sulfur that arises as a result of the degradation of sulfuric amino acids into smaller components. Therefore, finding a use for jengkol peels waste requires balancing technological advancement, financial viability, and environmental concern. It employed jengkol peels as a carbon source to synthesized CDs, which helped it dispose of jengkol peels waste more effectively.

One drawback is that CDs produced from natural precursors exhibit quantum fluorescence intensities that are ~10% less (Haochi et al., 2019) compared to metal-based quantum dot semiconductors, this affects the sensitivity of the synthesized CDs in sensing applications. The mechanism of fluorescence in CDs is related to its surface state, which includes defects and functional groups (Liu et al., 2020) (Ding et al., 2020) (Wang et al., 2017). In CDs synthesis, the CDs surface is covered by various hydrophilic groups such as —OH,—C═O or —COOH (Ding et al., 2020). These groups allow CDs to be surface functionalized. by adding heteroatoms so as to increase the fluorescence properties and the resulting quantum yield. This allows CDs to undergo surface functionalization –N, C, B heteroatom doping (Sun and Lei, 2017). Nitrogen is often used as a dopant because of its valence electrons, atomic size which is not much different from the carbon atoms that it can be connected to easily into the framework of the carbon material (Yan et al., 2019) and N doping may also act as an electron donor that increases fermi energy levels.

To date, the fluorescence properties of heteroatom-doped CDs have been developed as a sensor material for detecting the presence of heavy metal ions content such as mercury (Hg^{2+}) (Yongli Liu et al., 2022) (Zhou et al., 2022) (Korah et al., 2022). Therefore, the potential for employing CDs as accurate, sensitive, and efficient materials for detecting mercury metal ion content is relatively high. This synthesis of CDs from jengkol peels is described in this study. The CDs is prepared with a target application as a sensor that exhibits fluorescence upon interaction with heavy metal Hg^{2+} ions.

2. Materials and methods

2.1. Materials

Jengkol peels were taken from Sumatera Utara Province, Indonesia. Ethanol (C_2H_6O 97%) and 18.2 MΩ/cm of deionized water were bought from CV. Rudang Jaya, Indonesia. Ethylenediamine ($C_2H_4(NH_2)_2$ 98 wt %), standard solution of Cobalt (II) nitrate ($Co(NO_3)_2$); Mercury (II) nitrate ($Hg(NO_3)_2$); Iron(II) nitrate ($Fe(NO_3)_2$); Zinc (II) nitrate ($Zn(NO_3)_2$); Nickel (II) nitrate ($Ni(NO_3)_2$); Manganese (II) nitrate ($Mn(NO_3)_2$); Copper (II) nitrate ($Cu(NO_3)_2$); Cadmium II) nitrate ($Cd(NO_3)_2$); Lead (II) nitrate ($Pb(NO_3)_2$); Chromium (II) nitrate ($Cr(NO_3)_2$) and Magnesium(II) nitrate ($Mg(NO_3)_2$) were bought from Merck in Germany. The majority of chemical reagents were of the pro-analysis variety and were utilized directly.

2.2. Jengkol peels extract

During the experiment, jengkol peels were cleansed with tap water, distilled water using tap water, and oven-dried at 60 °C. The dried peels were subsequently crushed into powder by pulverisation. Powdered peels were extracted with organic solvents (ethanol 97%) with an increase of polarity at a 1: 10 (w/v). The extractions were performed by maceration for the extract simplicial containing chemical components readily soluble in solvents.

2.3. Synthesis of carbon dots (CDs) and nitrogen-doped carbon dots (N-CDs)

Jengkol peels extract (50 mL) was placed into a 100 mL autoclave in a high-temperature reaction kettle lined with Teflon at 200 °C for 7 h. After cooling to room temperature, a brown mixture was obtained. This Browne suspension was centrifuged for 40 min at 5500 rpm to separate the solids containing CDs.

For the synthesis of N-CDs, jengkol peels extract (50 mL) was added to ethylenediamine (10 mL) in a beaker and stirred at 350 rpm for 15 min using a magnetic stirrer until the solution was homogenous. This solution was transferred to a similar autoclave and processing conditions as described above and have been presented in Fig. 1. a similar centrifuge and filtration process as CDs was also employed to obtain N-CDs.

2.4. Fluorescence quantum yield measurements

Quantum yield (QY) measurements of CDs and N-CDs are calculated using the following equation (1) from the literature (Yi et al., 2021):

$$QYc = QYs \times \frac{Ic}{Is} \times \frac{As}{Ac} \times \left(\frac{\eta c}{\eta s}\right)^2 \quad (1)$$

Quinine sulfate was chosen as the fluorescence reference (QY = 54% and η = 1.33), where QY is the quantum yield value. I is the area of integrated photoluminescence intensity, A is the absorbance value, and η is the refractive index of the solvent. The subscripts "c" and "s" refer to CDs and Quinine sulfate. The respective photoluminescence spectra were obtained from a Perkin Elmer fluorescence spectrometer (model LS45).

2.5. Characterization

High-resolution transmission electron microscopy (HR-TEM) was performed using a JEOL-2100 TEM (accelerating voltage of 200 kV) to characterize the CDs solution's morphology. The particle size of CDs was determined with image J software. Fourier- Transform Infrared Spectroscopy (FTIR) spectra were recorded to analyse surface functional groups CDs in 4000 cm^{-1} – 400 cm^{-1} at room temperature using a Perkin Elmer spectrometer. The sample's chemical analysis was investigated using X-Ray photoelectron spectroscopy (XPS) carried out using the Kratos Axis Supra and monochromatic Al-Kα radiation of 1,486.6 eV at 150 W. UV–Visible spectrophotometer by using a Shimadzu UV-1800 in the range 200–700 nm and the fluorescence photoluminescence spectrometer by using a Perkin Elmer LS45 were utilized to record the optical properties of various operations respectively.

2.6. Heavy metal ion detection

The detection and selectivity of Hg^{2+} in the presence of various heavy metal ions was evaluated based on the quenched fluorescence-phenomenon. N-CDs solution (2 mL) was mixed with 100 μM concentration of each the heavy metal ions, including Co^{2+}, Hg^{2+}, Fe^{2+}, Zn^{2+}, Ni^{2+}, Mn^{2+}, Cu^{2+}, Cd^{2+}, Pb^{2+}, Cr^{2+} and Mg^{2+}. The sensitivity of Hg^{2+} ions was also analyzed by adding Hg^{2+} ion concentrations from 0,5 μM to 4.5 μM. the changes in the fluorescence intensity recorded in the fluorescence experiment were measured under the same conditions including room temperature, in each experiment, a 1:1 solution ratio was used (not only for N-CDs to interact with different metal ions, but also for N-CDs to interact with different amounts Hg^{2+}) and before the 370 nm fluorescence measurement was taken, each mix was given a gentle stir for 15 min.

To evaluate the detection Hg^{2+} sensitivity in a real-life scenario. Cosmetics (Toner) and tap water samples were selected. All samples were filtered and centrifuged at 5500 rpm for 15 min. Each resulting

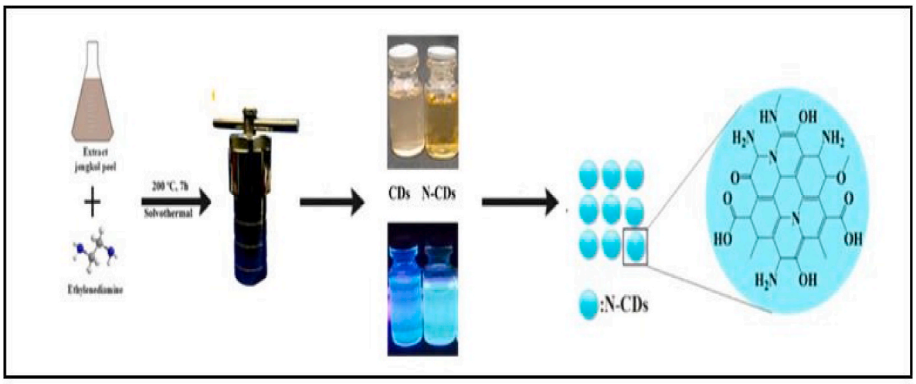

Fig. 1. The method used to the preparation N-CDs from jengkol peels.

supernatant were spiked with Hg^{2+} ions at various concentration levels and stirred for 10 min. Then, using the general procedure, followed by analysis using the proposed method.

3. Results and discussion

3.1. Characterization of carbon dots (CDs) and nitrogen-doped carbon dots (N- CDs)

The morphology and size distribution of the CDs and N-CDs were analyzed using HR-TEM which is seen in Fig. 2. The HR-TEM of the CDs shown in Fig. 2 (a,c) exhibit a spherical (dot), small, monodisperse shape without aggregates and having a size distribution of 1–8 nm. From the results of calculating the average sizes of CDs particles from jengkol peels using the image j application is 3,927 nm. Previous research also obtained carbon dots particle diameter of 5.0 nm from biomass (Pang et al., 2022), this proves that jengkol peels biomass can be a source of carbon dots precursors that has a particle size distribution less than 10 nm.

whereas HR-TEM of N-CDs Fig. 2 (b,d) shows a spherical, small, monodispersed CDs without any aggregation with size distribution (average size 4.495 nm). This shows that the addition of N Dopants can increase the particle size, and the two samples are consistent with the size distribution of nanoscale CDs that have been obtained in the literature (Torres Landa et al., 2022), and from the results of calculations using image J software, the lattice spacing of 0.24 nm CDs and N-CDs is obtained (inset of Fig. 2a and b), which is the distance between the carbon layers (100) of graphene (Z. Wang et al., 2020). These results indicate that both samples consist of amorphous and crystalline parts composed of carbon sp^2 graphite.

The functional groups present on CDs and N-CDs are shown in Fig. 3. All samples have a wide peak at 3291 cm^{-1} associated with OH stretching vibration (Liu et al., 2023), a peak at 2938 cm^{-1} – 2835 cm^{-1}

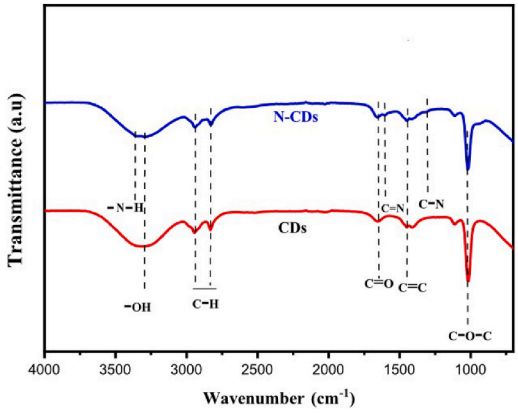

Fig. 3. FTIR spectrum of CDs and N-CDs.

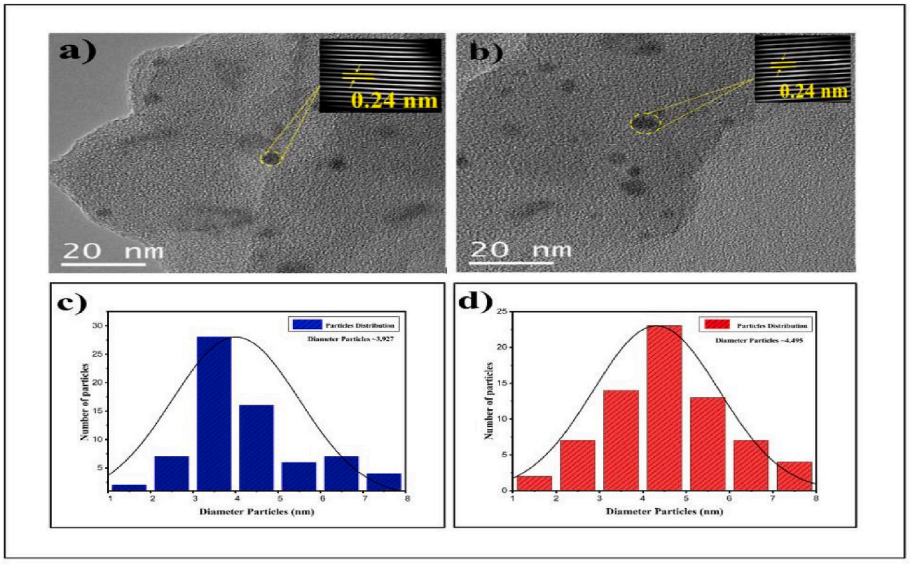

Fig. 2. HR-TEM morphology and lattice spacing of CDs (a) and N-CDs (b), Particle size distribution of CDs (c) and N-CDs (d).

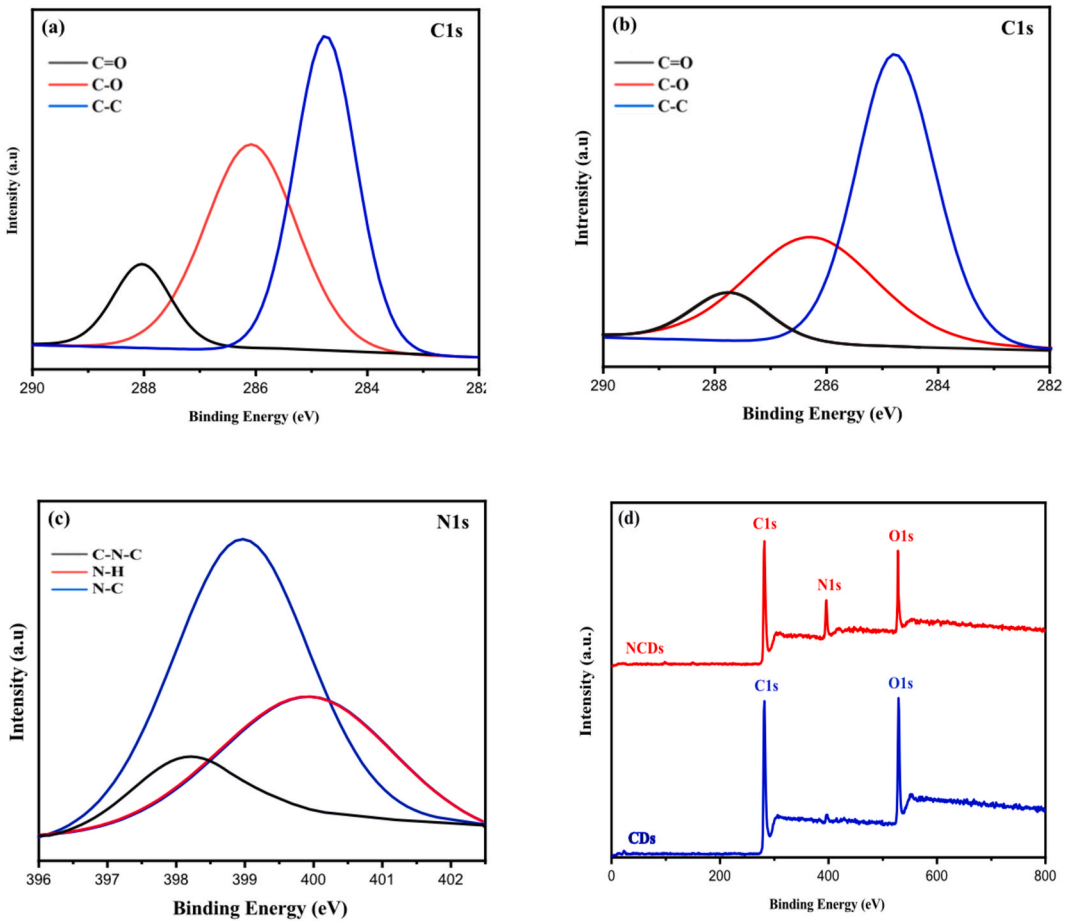

Fig. 4. XPS spectra high-resolution C1s of (a) CDs, (b) N-CDs, (c) XPS spectra high-resolution N1s of N-CDs and (d) XPS spectrum of the CDs and N-CDs samples.

belongs to C–H stretching vibration (Zhou et al., 2022), the C═O bond may also be present due to the presence of the absorption peak 1646 cm^{-1} (Zhou et al., 2023), while the peak of 1445 is caused by the C═C stretching vibration in the aromatic ring structure (Deng et al., 2018), and the sharp peak at 1025 cm^{-1} that is largely associated to the C–O–C stretching vibrations (Tony Elizabeth et al., 2023) is characteristic of CDs formation. N-CDs is the only sample that has N–H, C–N, and C═N bondings present in the spectra at absorption peaks of 3286 cm^{-1} (Liu et al., 2023), 1304 cm^{-1} (Yinghui et al., 2022), and 1608 cm^{-1} (Zhou et al., 2022), respectively. Which proves that the Heteroatom N is successfully doped in the carbon dot structure. The existence of oxygenated functional groups causes CDs and N-CDs to exhibit hydrophilicity that can increase their affinity to water. Therefore, it can be concluded that CDs and N-CDs have a polyaromatic structure because they contain carboxyl, hydroxyl, and N-CDs only sample that has amines.

Elemental composition and chemical structure analysis was further characterized using the XPS instrument. Fig. 4 shows that the CDs and N-CDs have little differences for the high-resolution spectra of C1s consisting of three peaks, including binding energy (BE) of 284.4 eV associated with C═C, the chemical bond originating from sp^2 C═O is at binding energy (BE) 288.9 eV and sp^3 C–O appeared at 286.6 eV (Qi et al., 2019). The C═C bond signal proves that both samples have gone through the carbonization process. For the high-resolution spectrum of N1s found only on N-CDs exhibiting three distinct peaks at binding energies of 398.5 eV, 399.1 eV, and 400.2 eV, respectively, these three groups are called pyridinic N; amine and pyrrolic N which are suspected from the C═N aromatic group of N-CDs (Kan et al., 2019). Moreover, the configurations of C–N in CDs can significantly influence the PL intensity due to the effect of delocalized electrons from pyridinic N. Those results showed that the N- CDs have hydrophilic groups like OH, COOH, NH_2, and O–C–O bonds on their surfaces. This gives the N- CDs good water solubility for different uses.

3.2. *Optical properties of carbon dots (CDs) and nitrogen-doped carbon dots (N- CDs)*

The optical absorption characteristics of CDs and N-CDs were evaluated through the UV–Visible and PL spectra which can be seen in Fig. 5. The inset in Fig. 5a shows that the as-synthesized CDs and N-CDs have high dispersion in aqueous solution and emit intense bluish-green fluorescence when exposed to a UV light with a wavelength of 365 nm. Clearly, as seen in Fig. 5a, there is a UV–Visible spectra of CDs and N-CDs have absorbance peaks at 286 nm and 284 nm, respectively, which are (Qi et al., 2019) ascribed to the π-π* transition for the ring aromatic C═C bond in the carbon core, and the absorbance at 397 nm is attributed to the transition n-π* (Kan et al., 2019) taking place between the C═O and C═N groups that collect on the surface and is only present on N-CDs. The change in the absorbance intensities and profile in N-CDs is hypothesized to be due to changes in the energy levels of the carbon dots after and before doped.

The PL spectra (Fig. 5b) explained that the PL intensities of all CDs and N-CDs samples showed maximum emission peaks at 497 nm and 522 nm. It can be seen in the PL N-CDs spectrum that the addition of nitrogen dopants to the carbon dots causes a red shift. The resulting PL intensity of N-CDs(Fig. 5b) is much higher than that of CDs, which is thought to be the result of nitrogen doping which forms defects in the N-CDs structure. This suppresses the number of O-states on the N-CDs surface and facilitates better radiative electron hole recombination so that the resulting PL intensity increases. Fig. 5c and d shows a fluorescence spectrum at various excitation wavelengths, and it can be shown

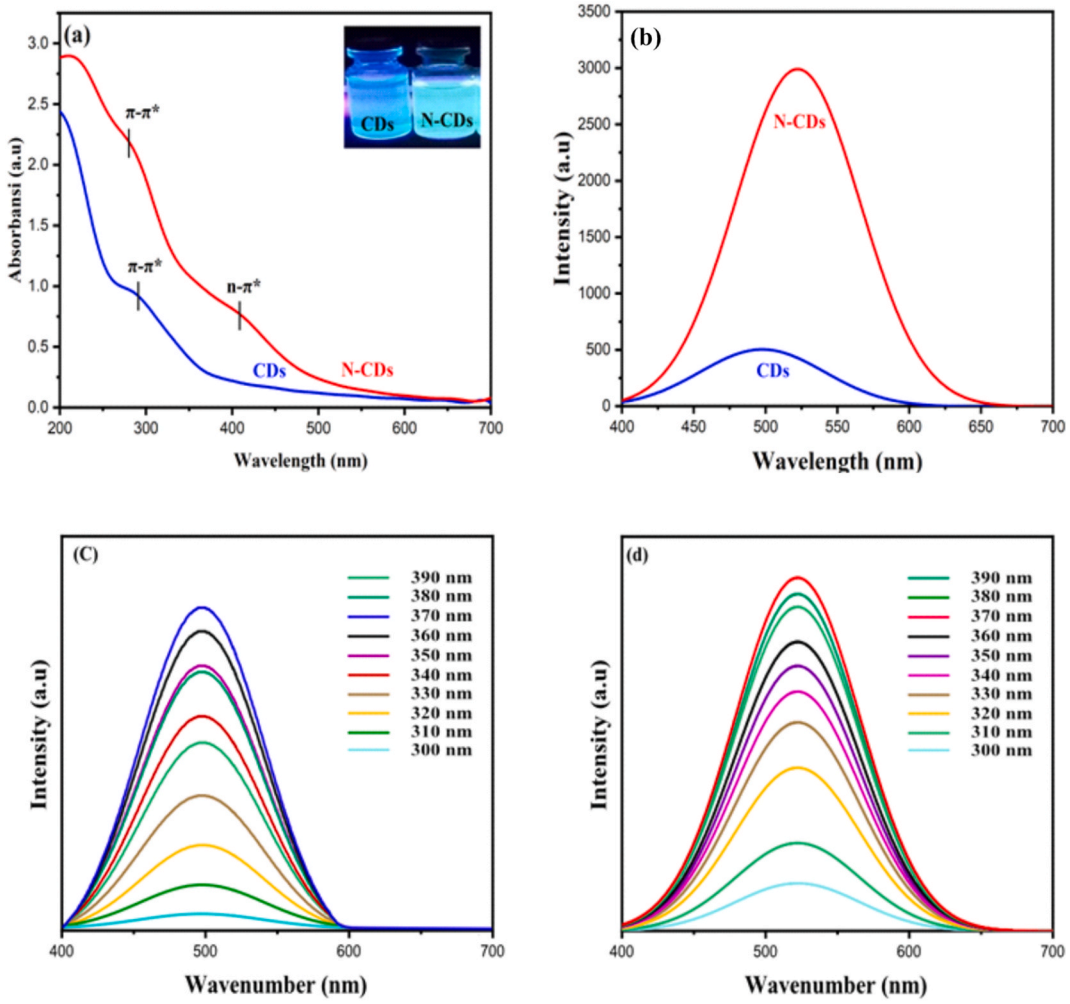

Fig. 5. (a) UV–Vis absorption spectrum of CDs and N-CDs, (b) The fluorescence spectra of CD_s and N-CD_s, (c) CD_s, and (d) N-CD_s that are excited (λ_{ex}) with different wavelengths.

that CDs and N- CDs has a specific excitation - optimum dependency and excitation wavelength 370 nm. where most of the particles are excited and the PL intensity of N-CDs turns out to be the highest. This is due to the presence of different functional groups on the surface of the CDs, there may be a series of emissive traps between π-π* from C═C (Molaei, 2019) and has been observed to increase the quantum yield (Yan et al., 2019) in N-CDs (42%) while CDs (24%). Because of the high fluorescence intensity and resultant quantum yield, N-CDs can be employed as a fluorescence probe to detect heavy metal ions.

3.3. Selectivity and sensitivity of N-CDs for Hg^{2+} detection

Highly fluorescence and great stability were seen in the NCDs that were produced. The high N-CDs fluorescence emission is caused by surface conditions associated with functional groups and surface oxidation. If the level of surface oxidation increased, the surface defect would intensify significantly. When nitrogen with functional groups is added to the surface, defect sites may result. Due of the excitons' radiative recombination, these defect sites caused trapped fluorescence emission. Fluorescence property was utilized to evaluate the ability of N-CDs to detect Hg^{2+} metal ions. Fig. 6 shows the variation in fluorescence intensity of different heavy metal ions used in the N-CDs selectivity test, including Ni^{2+}, Mn^{2+}, Hg^{2+}, Zn^{2+}, Co^{2+}, Pb^{2+}, Zn^{2+}, Fe^{2+} and Cu^{2+} at a concentration of 100 μM. Hg^{2+} ions showed the lowest fluorescence intensity while adding Ni^{2+}, Mn^{2+}, Hg^{2+}, Zn^{2+}, Co^{2+}, Pb^{2+}, Zn^{2+}, Fe^{2+} and Cu^{2+} ions had no significant effect on the fluorescence intensity of N-CDs. Thus demonstrating the selectivity that N-CDs have towards Hg^{2+} ions. This may be due to the presence of Hg^{2+} ions in solution quenched the fluorescence intensity (F_0/F) of N-CD_s at an excitation wavelength of 370 nm. According to Xu nitrogen-doped carbon dots contain functional groups that are sensitive to Hg^{2+} ions such as –OH, $–NH_2$, and COOH on the surface, that have high affinity to the d-orbitals belonging to Hg^{2+} ions, which would lead to the formation of non-fluorescent complexes (Xu et al., 2021b). Metal ions evaluated may participate in limiting the fluorescence quenching due to their interaction with electron donor groups present on carbon dots (Zhang et al., 2018).

The sensitivity of the ability of N-CDs to detect Hg^{2+} ions was also evaluated. The fluorescence intensity decreased in a linear fashion with increasing Hg^{2+} ion concentration in 0.5 μM–4.5 μM as shown in Fig. 6 (c,d) N-CDs is shown to be capable of Hg^{2+} ions at the limit of detection (LOD) of 0.03 μM with $R^2 \sim 0.99$. In order to check the stability of N-CDs, the storage time on the fluorescence property of N-CDs was investigated, the results showed the CDs solution remained in a homogeneous phase for 60 days, this indicated the long-term stability of the synthesized N-CDs.

This study resulted in a lower detection limit than the previous carbon dots fluorescence sensors, which are detailed in Table 1. Furthermore, it shows that N-CDs are extremely sensitive to the presence of Hg^{2+} ions and better than other semiconductor quantum dots even other organic dyes in detecting metallic Hg^{2+} ions because in addition to using non-toxic biomass as a carbon source, primary amines are also

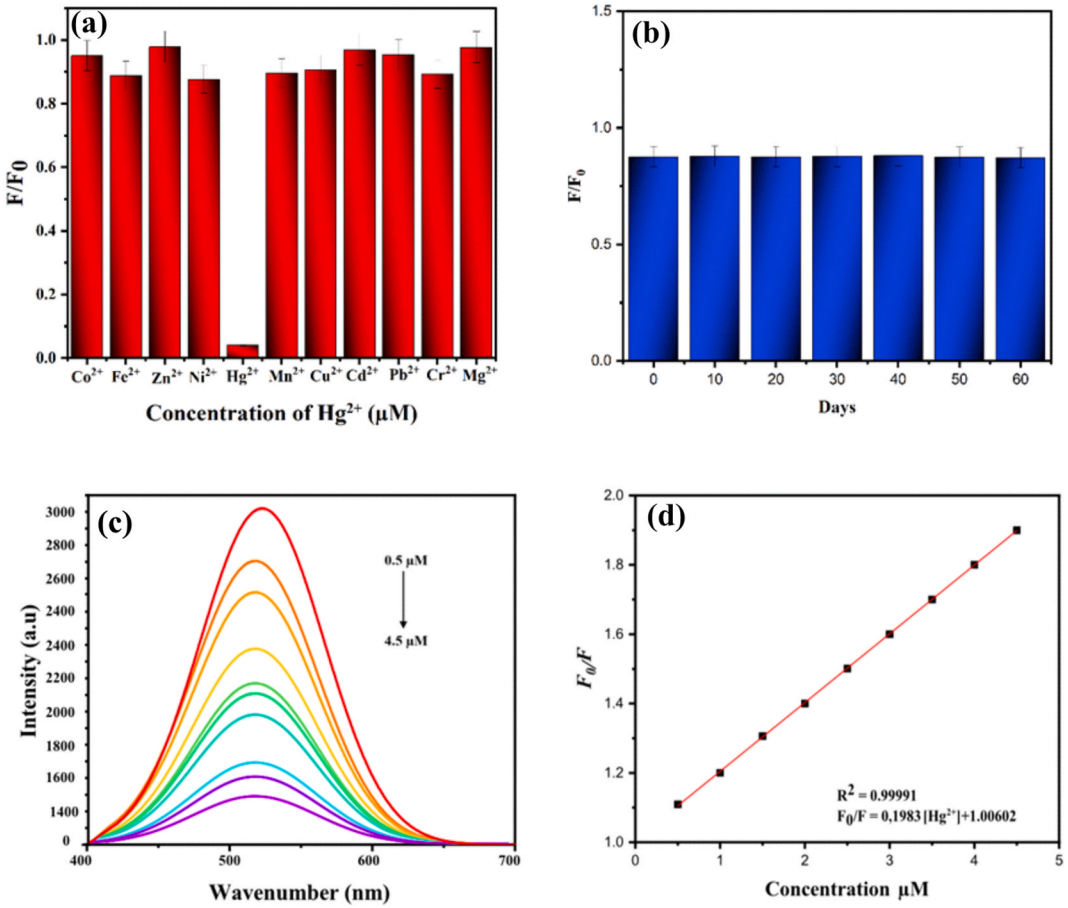

Fig. 6. (a) Fluorescence changes as a result of the addition of various heavy metal ions, (b) Storage time, (c) Spectrum of decreasing N-CDs fluorescence intensity based on adding Hg^{2+}, and (d) Linearity graph between the level of Hg^{2+} and the intensity of N-CDs fluorescence.

Table 1
Comparison of the proposed study in comparison to previously reported Hg^{2+} ions and detection methods in the literature.

Object of Detection	Method of Detection	Linear range (μM)	LOD (μM)	Reference
Hg^{2+}	Natural Phenol derivates	0.25-8	0.10	Zhang et al. (2018)
	Rhodamine B	0.11-200	0.11	Kan et al. (2019)
	AuNPs	0.2-20	0.06	(Liu et al., 2018)
	M-CDs	0-1.0	0.05	Li et al. (2020)
	N-CDs	0-200	0.96	(Xu et al., 2021a)
	N-CDs	20-150	0.12	(Liu et al., 2022)
	B–N-CDs	0-150	2.50	Meng et al. (2022)
	N-CDs	0.5-4.5	0.03	This work

employed as nitrogen sources. Based on their chemical structure, secondary and tertiary amines are thought to be able to lower the density of the electron cloud on the benzene ring, making them more difficult to quench N- CDs than primary amines.

3.4. Real sample test

The observation of the performance of N-CDs was applied to cosmetic samples (toner) and tap water. It is known that the concentration of Hg^{2+} ions in each cosmetic (1, 2 and 3 μM) was added to the N-CDs solution, and the PL intensity was recorded. The results revealed that Hg^{2+} ions recovery in the sample was around 92–95% with relative standard deviations (RSD, n = 3) less than 3.5%, while the concentration of tap water (1.5, 2.5, and 3.5 μM) was added to the N-CDs solution, and the PL intensity was recorded. The results revealed a recovery of Hg^{2+} ions in the sample of about 98.57–106.67% (RSD, less than 2.5%). The results of the research (Table 2) show that N-CDs are suitable for detecting Hg^{2+} ions using the fluorescence technique, which can be applied in various environments.

4. Conclusion

The Highly fluorescent N-CDs were successfully synthesized from jengkol peels band ethylenediamine by solvothermal method. The resulting N-CDs emit bluish-green fluorescence with a QY value of 42%. In addition, N-CDs are spherical and agglomerated with an average size of 4.495 nm and a lattice spacing of 0.24 nm. N-CDs contain poly aromatic groups which were confirmed from FTIR analysis and The XPS spectrum includes C–N–C (399.16 eV), N–H (400.2 eV), and C═N

Table 2
Hg^{2+} ions analysis in actual samples.

Samples	Spiked (μM)	Detected (μM)	Recovery (%)	RSD (%, n = 3)
Cosmetic	1	0.93	93	1.06
	2	1.90	95	1.38
	3	2.76	92	1.09
Tap water	1.50	1.60	106.67	2.23
	2.50	2.48	99.20	1.02
	3.50	3.45	98.57	1.01

(398.5 eV) peaks. Based on its excellent water solubility and The high fluorescence of N-CDs can improve the detection ability of Hg^{2+} metal ions from N-CDs. The fluorescence intensity of N-CDs decreased significantly when the Hg^{2+} Metal Ion concentration increased. The limit of detection (LOD) of 0.03 μM ranges from 0.5 to 4.5 M and is applied to detect Hg^{2+} ions in cosmetics and tap water.

CRediT authorship contribution statement

Aniza Salviana Prayugo: Writing – original draft, Editing. **Marpongahtun:** Investigation, Conceptualization. **Saharman Gea:** Investigation, Methodology. **Amru Daulay:** Review, Investigation. **Mahyuni Harahap:** Visualization. **Jonathan Siow:** Data curation. **Ronn Goei:** Data curation, Validation. **Alfred Iing Yoong Tok:** Data curation.

Declaration of competing interest

The authors declare that they have no known competing financial interests or personal relationships that could have appeared to influence the work reported in this paper.

Data availability

Data will be made available on request.

Acknowledgments

The Ministry of Research, Technology and Higher Education, Republic of Indonesia, supports this study (PTM 2022 research grant no.037/un5.3.2.1/PPM/KP-DRTPM/TI/2022).

References

Alkian, I., Sutanto, H., Hadiyanto, B., Prasetio, A., Aprimanti Utami, B., 2022. Facile synthesized carbon dots for simple and selective detection of cobalt ions in aqueous media. Cogent Eng. 9 (1).

Chao-Mujica, F.J., Garcia-Hernández, L., Camacho-López, S., Camacho-López, M., Camacho-López, M.A., Reyes Contreras, D., Pérez-Rodríguez, A., Peña-Caravaca, J. P., Páez-Rodríguez, A., Darias-Gonzalez, J.G., Hernandez-Tabares, L., Arias de Fuentes, O., Prokhorov, E., Torres-Figueredo, N., Reguera, E., Desdin-García, L.F., 2021. Carbon quantum dots by submerged arc discharge in water: synthesis, characterization, and mechanism of formation. J. Appl. Phys. 129 (16).

Deng, X., Feng, Y., Li, H., Du, Z., Teng, Q., Wang, H., 2018. N-doped carbon quantum dots as fluorescent probes for highly selective and sensitive detection of Fe3+ ions. Particuology 41, 94–100.

Dhanush, C., Aravind, M.K., Ashokkumar, B., Sethuraman, M.G., 2022. Synthesis of blue emissive fluorescent nitrogen doped carbon dots from Annona squamosa fruit extract and their diverse applications in the field of catalysis and bio-imaging. J. Photochem. Photobiol. Chem. 432 (3), 114097.

Ding, H., Li, X.H., Chen, X.B., Wei, J.S., Li, X.B., Xiong, H.M., 2020. Surface states of carbon dots and their influences on luminescence. J. Appl. Phys. 127 (23).

Goei, R., Tan, F.T.F., Ong, A.J., Mandler, D., Tok, A.I.Y., 2022. Development of nitrogen-decorated carbon dots (NCDs) thermally conductive film for windows application. Carbon Lett. 32 (4), 1065–1072.

González-González, R.B., González, L.T., Madou, M., Leyva-Porras, C., Martinez-Chapa, S.O., Mendoza, A., 2022. Synthesis, purification, and characterization of carbon dots from non-activated and activated pyrolytic carbon black. Nanomaterials 12 (3).

Kaczmarek, A., Hoffman, J., Morgiel, J., Mościcki, T., Stobiński, L., Szymański, Z., Małolepszy, A., 2021. Luminescent carbon dots synthesized by the laser ablation of graphite in polyethylenimine and ethylenediamine. Materials 14 (4), 1–13.

Kan, C., Shao, X., Song, F., Xu, J., Zhu, J., Du, L., 2019. Bioimaging of a fluorescence rhodamine-based probe for reversible detection of Hg (II) and its application in real water environment. Microchem. J. 150, 104142.

Kang, C., Huang, Y., Yang, H., Yan, X.F., Chen, Z.P., 2020. A review of carbon dots produced from biomass wastes. Nanomaterials 10 (11), 1–24.

Korah, B.K., Punnoose, M.S., Thara, C.R., Abraham, T., Ambady, K.G., Mathew, B., 2022. Curcuma amada derived nitrogen-doped carbon dots as a dual sensor for tetracycline and mercury ions. Diam. Relat. Mater. 125 (1), 108980.

Li, D.Y., Wang, S.P., Azad, F., Su, S.C., 2020. Single-step synthesis of polychromatic carbon quantum dots for macroscopic detection of Hg(II). Ecotoxicol. Environ. Saf. 190, 110141.

Liu, Huadong, Li, H., Du, K., Xu, H., 2022. Yellow fluorescent carbon dots sensitive detection of Hg^{2+} and its detection mechanism. Mater. Today Commun. 33 (10), 104880.

Liu, J., Li, R., Yang, B., 2020. Carbon dots: a new type of carbon-based nanomaterial with wide applications. ACS Cent. Sci. 6 (12), 2179–2195.

Liu, K., Xia, C., Guo, Y., Yu, H., Xie, Y., Yao, W., Xia, C., Guo, Y., Yu, H., Xie, Y., Yao, W., 2023. Polyethylenimine-functionalized nitrogen and sulfur co-doped carbon dots as effective fluorescent probes for detection of Hg2+ ions Kunfeng. Spectrochica Acta 292 (5), 122395.

Liu, Yan, Ouyang, Q., Li, H., Chen, M., Zhang, Z., Chen, Q., 2018. Turn-on fluoresence sensor for Hg^{2+} in food based on FRET between aptamers-functionalized upconversion nanoparticles and gold nanoparticles. J. Agric. Food Chem. 66 (24), 6188–6195.

Liu, Yinghui, Yong, C., Tong, B., Li, Y., Wang, N., Lei, Y., 2022. Modification of carbon dots derived from biomass by exogenous nitrogen doping: action mechanism and difference analysis. Opt. Mater. 134 (10).

Liu, Yongli, Zhou, P., Wu, Y., Su, X., Liu, H., Zhu, G., Zhou, Q., 2022. Fast and efficient "on- off-on" fluorescent sensor from N-doped carbon dots for detection of mercury and iodine ions in environmental water. Sci. Total Environ. 827, 154357.

Marpongahtun, Andriayani, Muis, Y., Gea, S., Amaturrahim, S.A., Attaurrazaq, B., Daulay, A., 2023. Synthesis of nitrogen-doped carbon dots from nanocrystalline cellulose by pyrolysis method as Hg^{2+} detector. Int. J. Technol. 14 (1), 219–231.

Meng, A., Zhang, Y., Wang, X., Xu, Q., Li, Z., Sheng, L., Yan, L., 2022. Fluorescence probe based on boron-doped carbon quantum dots for high selectivity "on-off-on" mercury ion sensing and cell imaging. Colloids Surf. A Physicochem. Eng. Asp. 648, 129150.

Molaei, M.J., 2019. A review on nanostructured carbon quantum dots and their applications in biotechnology, sensors, and chemiluminescence. Talanta 196, 456–478.

Nadira Hurairah, S., Mohamad Fahimi, N.S., Abdul Halim, A., Mohd Hanafiah, M., Nordin, N., Ain Ab Jalil, N., Daud, Z., 2023. Archidendron jiringa seed peel extract in the removal of lead from synthetic residual water using coagulation-flocculation process. Sci. Asia 49 (1), 94.

Pang, Z., Fu, Y., Yu, H., Liu, S., Yu, S., Liu, Y., Wu, Q., Liu, Y., Nie, G., Xu, H., Nie, S., Yao, S., 2022. Efficient ethanol solvothermal synthesis of high-performance nitrogen-doped carbon quantum dots from lignin for metal ion nanosensing and cell imaging. Ind. Crop. Prod. 183, 114957.

Pramudita, R., Marpongahtun, Gea, S., Daulay, A., Harahap, M., Tan, Y.Z., Goei, R., Tok, A.I.Y., 2022. Synthesis of fluorescent citric acid carbon dots composites derived from empty fruit bunches of palm oil tree and its anti-bacterial property. Case Stud. Chem. Environ. Eng. 6 (1), 100277.

Qi, H., Teng, M., Liu, M., Liu, S., Li, J., Yu, H., Teng, C., Huang, Z., Liu, H., Shao, Q., Umar, A., Ding, T., Gao, Q., Guo, Z., 2019. Biomass-derived nitrogen-doped carbon quantum dots: highly selective fluorescent probe for detecting Fe^{3+} ions and tetracyclines. J. Colloid Interface Sci. 539, 332–341.

Rahmayanti, M., Nurul Syakina, A., Fatimah, I., Sulistyaningsih, T., 2022. Green synthesis of magnetite nanoparticles using peel extract of jengkol (Archidendron pauciflorum) for methylene blue adsorption from aqueous media. Chem. Phys. Lett. 803, 139834.

Sun, X., Lei, Y., 2017. Fluorescent carbon dots and their sensing applications. TrAC, Trends Anal. Chem. 89, 163–180.

Tony Elizabeth, A., James, E., Infant Jesan, L., Denis Arockiaraj, S., Edwin Vasu, A., 2023. Green synthesis of value-added nitrogen doped carbon quantum dots from Crescentia cujete fruit waste for selective sensing of Fe^{3+} ions in aqueous medium. Inorg. Chem. Commun. 149 (January), 110427.

Torres Landa, S.D., Reddy Bogireddy, N.K., Kaur, I., Batra, V., Agarwal, V., 2022. Heavy metal ion detection using green precursor derived carbon dots. iScience 25 (2), 103816.

Villalba-Rodríguez, A.M., González-González, R.B., Martínez-Ruiz, M., Flores-Contreras, E.A., Cárdenas-Alcaide, M.F., Iqbal, H.M.N., Parra-Saldívar, R., 2022. Chitosan- based carbon dots with applied aspects: new frontiers of international interest in a material of marine origin. Mar. Drugs 20 (12), 1–14.

Wang, R., Lu, K.-Q., Tang, Z.-R., Xu, Y.-J., 2017. Recent progress on carbon quantum dots: synthesis, properties and applications in photocatalysis. J. Mater. Chem. 5.

Wang, Z., Chen, D., Gu, B., Gao, B., Wang, T., Guo, Q., Wang, G., 2020. Biomass-derived nitrogen doped graphene quantum dots with color-tunable emission for sensing, fluorescence ink and multicolor cell imaging. Spectrochim. Acta Mol. Biomol. Spectrosc. 227, 117671.

Wardani, G.A., Nuramalia, L., Wulandari, W.T., Nofiyantib, E., 2020. Lead (II) Ions Bio - sorbent with Column Method H 23 (85), 160–166.

Xu, D., Fu, N., Xie, Y., Wang, Y., Xie, R., Yang, H., Sun, W.L., Liu, X., Han, A., 2021a. Easy formation of nitrogen-doped carbon dots towards Hg2+ fluorescent measurement and multicolor intracellular imaging. Mater. Chem. Phys. 266 (8), 124547.

Xu, D., Fu, N., Xie, Y., Wang, Y., Xie, R., Yang, H., Sun, W., Liu, X., Han, A., 2021b. Easy formation of nitrogen-doped carbon dots towards Hg^{2+} fluorescent measurement and multicolor intracellular imaging. Mater. Chem. Phys. 266, 124547.

Xu, X., Ray, R., Gu, Y., Ploehn, H.J., Gearheart, L., Raker, K., Scrivens, W.A., 2004. Electrophoretic analysis and purification of fluorescent single-walled carbon nanotube fragments. J. Am. Chem. Soc. 126 (40), 12736–12737.

Yan, F., Sun, Z., Zhang, H., Sun, X., Jiang, Y., Bai, Z., 2019. The fluorescence mechanism of carbon dots, and methods for tuning their emission color: a review. Microchim. Acta 186 (8), 583.

Yi, Z., Li, X., Zhang, H., Ji, X., Sun, W., Yu, Y., Liu, Y., Huang, J., Sarshar, Z., Sain, M., 2021. High quantum yield photoluminescent N-doped carbon dots for switch sensing and imaging. Talanta 222, 121663.

Zhang, X., Guo, X., Yuan, H., Jia, X., Dai, B., 2018. One-pot synthesis of a natural phenol derived fluorescence sensor for Cu(II) and Hg(II) detection. Dyes Pigments 155, 100–106.

Zhou, R., Chen, C., Hu, J., Liao, X., Hu, H., Tong, Z., Liang, J., Huang, F., 2022. The self-nitrogen-doped carbon quantum dots derived from Morus alba L. leaves for the rapid determination of tetracycline. Ind. Crop. Prod. 188 (2), 115705.
Zhou, Y., Chen, G., Ma, C., Gu, J., Yang, T., Li, L., Gao, H., Xiong, Y., Wu, Y., Zhu, C., Wu, H., Yin, W., Hu, A., Qiu, X., Guan, W., Zhang, W., 2023. Nitrogen-doped carbon dots with bright fluorescence for highly sensitive detection of Fe^{3+} in environmental waters. Spectrochim. Acta Mol. Biomol. Spectrosc., 122414
Zhu, P., Wang, S., Zhang, Y., Li, Y., Liu, Y., Li, W., Wang, Y., Yan, X., Luo, D., 2022. Carbon dots in biomedicine: a review. ACS Appl. Bio Mater. 5 (5), 2031–2045.